J Appl Physiol
88: 1581–1589, 2000.

Regional differences in serotonergic input to canine parasternal intercostal motoneurons

WEN-ZHI ZHAN,[1] CARLOS B. MANTILLA,[1] PHILLIP ZHAN,[1] ASAF BITTON,[1]
Y. S. PRAKASH,[1] ANDRE DE TROYER,[3] AND GARY C. SIECK[1,2]
Departments of [1]Anesthesiology and [2]Physiology and Biophysics, Mayo Clinic and Foundation, Rochester, Minnesota 55905; and [3]Laboratory of Cardiorespiratory Physiology and Chest Service, Erasme University Hospital, Brussels School of Medicine, 1070 Brussels, Belgium

Zhan, Wen-Zhi, Carlos B. Mantilla, Phillip Zhan, Asaf Bitton, Y. S. Prakash, Andre De Troyer, and Gary C. Sieck. Regional differences in serotonergic input to canine parasternal intercostal motoneurons. *J Appl Physiol* 88: 1581–1589, 2000.—There is a mediolateral gradient in activation of the parasternal intercostal (PI) muscle during inspiration. In the present study, we tested the hypotheses that serotonergic [5-hydroxytryptamine (5-HT)] input from descending central drive and/or intrinsic size-related properties of PI motoneurons leads to the differential activation of PI muscles. In dogs, PI motoneurons innervating the medial and lateral regions of the PI muscles at the T_3–T_5 interspaces were retrogradely labeled by intramuscular injection of cholera toxin B subunit. After a 10-day survival period, PI motoneurons and 5-HT terminals were visualized by using immunohistochemistry and confocal imaging. There were no differences in motoneuron morphology among motoneurons innervating the medial and lateral regions of the PI muscle. However, the number of 5-HT terminals and the 5-HT terminal density (normalized for surface area) were greater in motoneurons innervating the medial region of the PI muscle compared with the lateral region. These results suggest that differences in distribution of 5-HT input may contribute to regional differences in PI muscle activation during inspiration and that differences in PI motoneuron recruitment do not relate to size.

respiratory muscles; biogenic amines; spinal cord; neuromodulation; immunohistochemistry; confocal microscopy

SINCE THE ELECTROMYOGRAPHIC (EMG) studies performed by Taylor (38) in normal humans, it has been recognized that the parasternal intercostal (PI) muscles are activated during inspiration. Measurements of muscle length and rib displacement in dogs (5, 6, 8) and baboons (7) have established that the PI muscles play a major role in the rhythmic inspiratory elevation of the ribs and expansion of the rib cage; the contribution of the canine PI muscles to rib elevation during resting breathing has been estimated to be ~80% (5). Only recently was it appreciated that the inspiratory activation of the PI muscles is not uniform. Specifically, inspiratory activity occurs first and is greatest in the medial region of the PI muscles, situated in the vicinity of the sternum (9). Activity occurs later and decreases progressively toward the chondrocostal junction, such that the lateral region of the PI muscles, situated near the lateral end of the cartilage, remains inactive throughout inspiration, even when breathing is stimulated by an inspiratory mechanical load (9).

The medial and lateral regions of the PI muscle within a given segment also differ in the orientation of fibers relative to the sternum (9). Indeed, the acute angle between the sternum and muscle fibers increases gradually from medial to lateral regions. As a result, the medial region of the PI muscle has a greater inspiratory mechanical advantage (i.e., a high inspiratory effect on the lung), whereas the lateral region of the PI muscle has no inspiratory mechanical advantage at all (9, 27). Thus the distribution of inspiratory activity across different regions of the PI muscle is precisely matched with the distribution of mechanical advantage, which indicates an extraordinarily effective pattern of contraction. Proprioceptive mechanisms, including muscle spindle and Golgi tendon organ reflexes, are known to play little or no role in producing this pattern of contraction (10).

Motoneuron recruitment is determined by a combination of intrinsic membrane excitability and the quantity and quality of synaptic connections. Intrinsic membrane properties that determine excitability are related to motoneuron size (Henneman size principle) (13–15). Larger motoneurons have greater membrane surface area, higher membrane capacitance, and higher rheobase, which make them less excitable. Therefore, larger motoneurons have a higher recruitment threshold than do smaller motoneurons. To the best of our knowledge, there is no information available on size differences in medial vs. lateral PI motoneurons.

In addition, descending synaptic input can modulate the recruitment threshold of motoneurons. Serotonergic [5-hydroxytryptamine (5-HT)] synaptic input, especially that derived from the brain stem raphe nuclei, facilitates automatic rhythmic motor behaviors such as respiration (21, 22, 26, 28, 30, 35). Serotonergic raphe projections to spinal respiratory motoneurons, including intercostal motoneurons, have been demonstrated (16, 18, 19, 25, 31, 40, 41). There is also recent functional evidence that 5-HT increases intercostal muscle activity (11, 34). Thus there appears to be both

The costs of publication of this article were defrayed in part by the payment of page charges. The article must therefore be hereby marked "*advertisement*" in accordance with 18 U.S.C. Section 1734 solely to indicate this fact.

morphological and functional evidence suggesting 5-HT modulation of PI motoneuron activity.

Alternative, but not necessarily exclusive, hypotheses were evaluated in the present study: *1*) motoneurons innervating the medial vs. lateral region of the canine PI muscle are smaller, and *2*) the earlier recruitment of medial vs. lateral PI motoneurons reflects greater 5-HT synaptic input.

METHODS

Five mongrel dogs (body weights 25–30 kg) were anesthetized with methohexital (12 mg/kg) and isoflurane (1.5 × minimum alveolar anesthetic concentration), placed supine on the operating table, and intubated with a cuffed endotracheal tube. Different regions of the PI muscles were exposed after skin incision. To retrogradely label PI motoneurons, 30 μl of a solution containing 0.5% cholera toxin B subunit (CTB; List Biological Laboratories, Campbell, CA) and 0.5% 1,1′-dioctadecyl-3,3,3′,3′-tetramethylindocarbocyanine perchlorate (DiI; Molecular Probes, Eugene, OR) were injected into randomly selected sites in the PI muscle. On the right or left side, three to five spots were injected in either the medial or lateral regions from the third to fifth intercostal spaces (T_3–T_5). A schematic diagram showing injection sites is given in Fig. 1. The addition of DiI to the injected solution was necessary to localize retrogradely labeled PI motoneurons during initial tissue processing (see below). In the present study, EMG activity was not monitored. However, several previous studies have clearly demonstrated a mediolateral gradient of inspiratory EMG activity in the canine PI muscle (9, 10). The sites of injection in the present study corresponded to those locations with the highest and lowest levels of EMG activity observed in these previous studies. After injection, the incisions were sutured, and the animals were carefully monitored. The animals were administered antibiotic and analgesic agents for 5 days after surgery. All experimental procedures were approved by the Institutional Animal Care and Use Committee at Mayo Clinic, and they were in strict accordance with the American Physiological Society animal care guidelines.

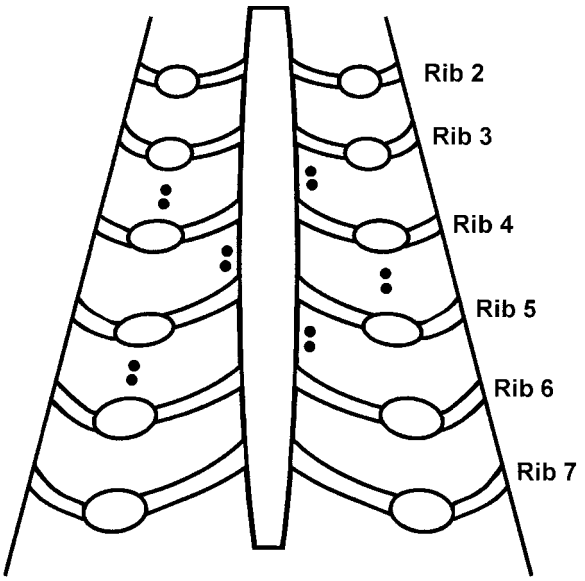

Fig. 1. Schematic diagram showing cholera toxin B subunit (CTB) injection sites used to retrogradely label parasternal intercostal motoneurons. Choice of medial vs. lateral regions for injection was random in each thoracic segment.

After a 10-day survival period, animals were anesthetized, and the sites of CTB injection into PI muscle regions were verified. Animals were then transcardially perfused with 4% paraformaldehyde in 0.1 M PBS, and the spinal cords were excised. After excision, the cords were marked with indelible ink to ensure proper orientation during sectioning. The tissues were kept in fixative overnight and then transferred to PBS for storage. The spinal cords were transversely sectioned at 150-μm thickness by using a vibratome (FHC, Brunswick, NJ).

Two-color immunohistochemistry. Sections of the spinal cord were initially screened under standard epifluorescence microscopy to identify those with DiI labeling. The DiI-positive sections were then immunohistochemically labeled for CTB and 5-HT. All procedures were performed at room temperature (25°C; pH 7.4). Sections were first blocked for 1 h in 5% normal donkey serum in 0.1 M Tris-buffered saline (0.15 M NaCl) containing 0.5% Triton X-100 (TBS-Tx). The samples were then incubated overnight (16–24 h) in a TBS-Tx solution containing 1:1,000 dilutions of goat IgG antibody to CTB (List Biologicals) and rabbit IgG antibody to 5-HT (IncStar, Stillwater, MN). After the primary antibody incubation, the sections were washed three times in TBS-Tx for 15 min each and then were incubated in a TBS-Tx solution containing 1:100 Cy3-conjugated donkey anti-goat IgG and Cy5-conjugated donkey anti-rabbit IgG (Jackson Immunoresearch, West Grove, PA) for 5–6 h. Accordingly, Cy3 and Cy5 labeled PI motoneuron somata and 5-HT boutons, respectively.

After the final incubation, the sections were thoroughly washed in TBS-Tx, and placed sequentially on a glass slide. Extreme care was taken to ensure that sections were consistently placed in the same orientation, i.e., ink marking to the right and the dorsal end toward the top. Sections were air dried and dehydrated in graded alcohol concentrations of 50, 90, and 100% for 5 min each. The slides were then coverslipped with histochemical mounting medium.

Confocal imaging. The techniques for three-dimensional (3D) confocal imaging have been described in detail previously (32, 36). Images were obtained by using a Bio-Rad MRC 600 (Bio-Rad, Hercules, CA) laser-scanning confocal microscope mounted on an Olympus BH2 microscope and equipped with an Ar-Kr laser. The 568- and 647-nm lines of the laser were used to excite the Cy3 and Cy5, respectively. Optical sections were obtained at 1.6-μm steps by using an Olympus DApo ×40 1.25-numerical aperature oil-immersion objective lens (768 × 512 pixels; resolution: XY ~0.4 μm; Z ~0.8 μm). The system was controlled by using manufacturer-supplied software. The Z-axis was controlled by a stepper motor (0.2 μm accuracy). Images of labeled PI motoneurons and 5-HT terminals were taken simultaneously by using double excitation, two fluorescence channels, and appropriate barrier filters.

Sections were first scanned by using low-power epifluorescence to select those with motoneuron soma. The sections within each segment were then imaged sequentially starting with the most rostral section. Only those motoneurons having somata that were completely within a physical section were imaged. Accordingly, motoneurons in which the nucleus was visible at the top or bottom of the section were ignored. For each motoneuron sampled, optical sections were obtained at an XY zoom of 3.0 (0.13 μm/pixel) and a Z-axis step size of 0.8 μm.

Morphometric analysis. For each animal, 175–200 motoneurons were imaged. Within each thoracic segment, at least 30

motoneurons were sampled. Given the large number of motoneurons, further analysis of the data was performed by using stereological sampling. Essentially, within each thoracic segment, every fifth motoneuron was selected for analysis, starting with a random initial selection. Overall, images from ~250 PI motoneurons were analyzed.

Sets of optical sections were transferred to ANALYZE, a comprehensive image-manipulation and -analysis software package (Mayo Biomedical Imaging Resource). Somal volumes and surface areas of motoneurons were measured from 3D reconstructions by using a voxel-connection surface-tracking algorithm.

The dendritic tree surface area was estimated as described by Burke et al. (1). In this analysis, the primary dendrite was identified from the stack of optical sections, and the initial diameter of each primary dendrite was measured at a point 15 μm from the soma. On the basis of this measurement, dendritic tree surface area was estimated by using the following formula

$$A_d = 986\ d_o^{1.88}$$

where A_d is the total dendrite membrane area of each dendrite and d_o is the primary dendrite diameter. The total motoneuron surface area was then estimated from the measured somal surface area and the sum of all individual dendritic surface areas.

Analysis of serotonergic synaptic input. Serotonergic boutons were identified in 3D from optical sections at 3.0 zoom, and those within 5 μm of the somata or dendrites were counted with a numerical tracker. Boutons occupying 9 pixels or fewer were counted as single entities. For clusters where individual boutons could not be identified, the number of boutons was estimated as the total pixel count for the cluster divided by nine. The density of 5-HT boutons was then obtained by normalizing the bouton count to the surface area of the individual PI motoneuron soma or dendrite. In addition, a random subset of dendritic branches was taken from the analyzed motoneurons to determine dendritic 5-HT density on the basis of dendritic branch order.

Statistical analysis. Morphological parameters were initially compared by using a two-way ANOVA with spinal cord segment and medial vs. lateral location as grouping variables. Statistical significance was tested at the 0.05 level. When appropriate, post hoc analyses were performed by using a Student-Newman-Keuls test.

RESULTS

Retrograde labeling of PI motoneurons. At the terminal experiment, the dye injection sites within the different PI muscle regions were confirmed. The marker was found to be well limited to the areas of injection. There was very little, if any, spread of the dye beyond 3–4 mm from the injection site, which was substantially smaller than the distance between medial and lateral aspects of the PI muscle. However, in one animal, both medial and lateral regions of the PI within the same segment appeared to be stained. Accordingly, the confocal data from motoneurons in the corresponding spinal cord segment were excluded from further analysis.

Motoneuron somata, proximal dendrites, and a significant portion of the distal dendritic tree were extensively and intensely labeled by CTB (Fig. 2). The dendrites were predominantly oriented toward the medial aspects of the gray matter, with several distal dendrites appearing to cross over to the contralateral ventral horn. Other dendrites were oriented dorsally and maintained a lateral track. Within each thoracic

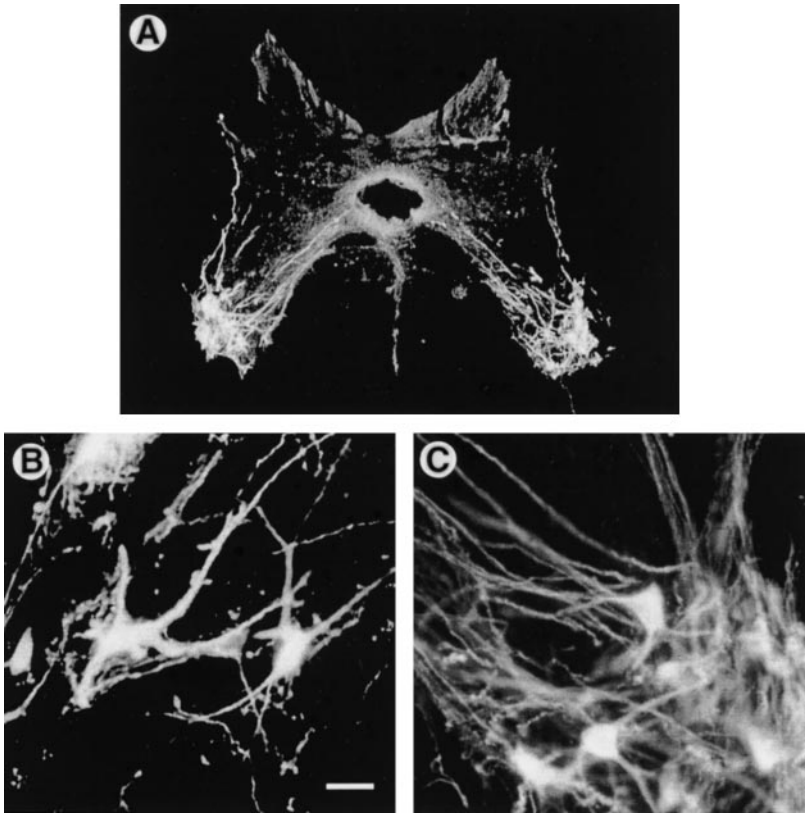

Fig. 2. CTB-labeled parasternal intercostal motoneurons in ventral horn of thoracic spinal cord. Representative example of a confocal projection image of parasternal intercostal motoneurons in segment T_4 is shown (*A*: ×100 magnification). Magnified views (×400 magnification) show motoneurons innervating medial (*B*) and lateral (*C*) aspects of parasternal intercostal muscle. Note extensive bilateral somatic and dendritic labeling of motoneurons. Also note lack of difference in position of motoneurons innervating medial vs. lateral aspects of muscle (*A*). Scale bars represent 150 μm in *A* and 35 μm in *B* and *C*.

segment, motoneuron somata appeared to form rostrocaudal clusters as indicated by the presence of soma in the groups of spinal cord sections, with intervening sections containing rostrocaudally oriented dendrites. The motoneuron clusters were separated rostrocaudally and located only at the spinal cord segments corresponding to the injected PI muscles, occupying <10% of each spinal cord segment. These results are consistent with previous reports indicating a segmentally concordant innervation of intercostal muscles (20). Further analysis was not possible by using transverse sections.

Location of PI motoneurons. Within a thoracic segment, PI motoneurons innervating the medial aspect of the muscle were distributed in both the medial and lateral aspects of the ventral horn (Fig. 2). Similarly, motoneurons innervating lateral aspects of the muscle were found distributed throughout the ventral horn. Systematic analysis of the location of motoneuron soma was performed by comparing the lateral distance and the dorsoventral distance between motoneurons and the most lateral point of gray matter (the reference point). Within a thoracic segment, there was no significant difference in either the lateral or dorsoventral distances of motoneurons innervating the medial vs. lateral aspects of the PI muscle (Fig. 3). There was also no significant difference in the location of motoneurons innervating the medial and lateral regions of PI muscles in different thoracic segments. Thus there was no significant correlation between motoneuron location in the spinal cord and the region of PI muscle innervated by the motoneuron.

Morphology of PI motoneurons. PI motoneuron soma displayed an elliptical profile in the *XY* plane. Measurements of the long- and short-axis dimensions were first used to estimate somal volume assuming a prolate spheroid (32). These estimates were 85–117% of corresponding measurements obtained from 3D volume reconstructions. Somal surface areas across segments and locations ranged from 4,100 to 5,000 μm^2. Somal volumes ranged from 20,800 to 28,700 μm^3.

Within a thoracic segment, there was no significant difference in the somal volume and somal surface area of motoneurons innervating the medial vs. lateral regions of the PI muscle (Fig. 4). Furthermore, across thoracic segments, there were also no differences in somal volume or somal surface area in either the medial or lateral aspects (Fig. 4).

The estimated dendritic surface areas varied considerably, ranging from 31,140 to 261,283 μm^2. Similarly, total motoneuron surface areas ranged from 35,231 to 267,032 μm^2. Dendritic and total PI motoneuron surface areas were not normally distributed but were unimodal (Fig. 5). The mean dendritic surface area was 115,538 ± 6,152 (SE) μm^2 in the medial group and 98,363 ± 4,500 μm^2 in the lateral PI motoneuron group. Median dendritic surface areas were 100,578 and 91,049 μm^2 in the medial and lateral PI motoneuron groups, respectively. The mean total surface area was 120,278 ±

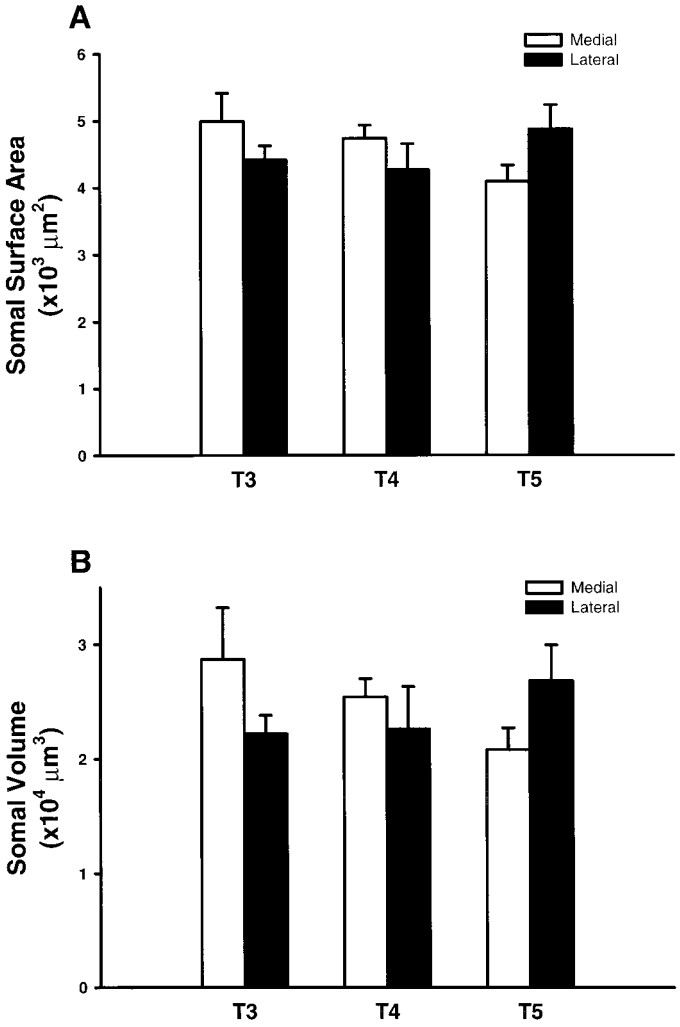

Fig. 4. Morphological measurements of parasternal intercostal motoneuron somata. Values are means ± SE. There are no significant differences in somal surface area (*A*) or somal volume (*B*) between motoneurons innervating medial and lateral portions of parasternal intercostal muscle ($P > 0.05$).

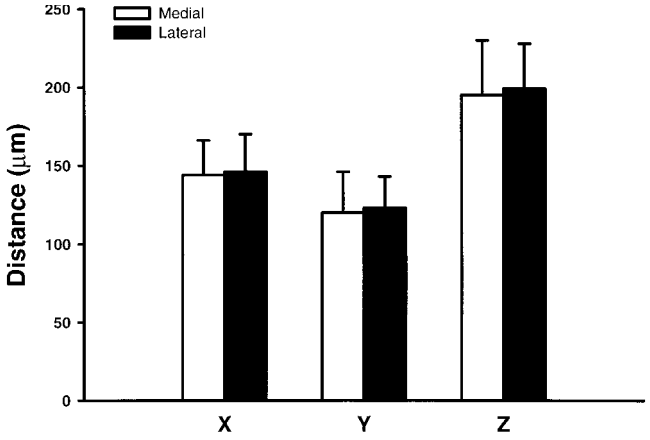

Fig. 3. Position of parasternal intercostal motoneurons in the ventral spinal cord. Lateral (*X*), dorsoventral (*Y*), and mean square (*Z*) distances were measured for motoneurons innervating medial vs. lateral aspects of parasternal intercostal muscle. Values are means ± SE. There are no significant differences in position of motoneurons innervating medial vs. lateral aspects across all segments.

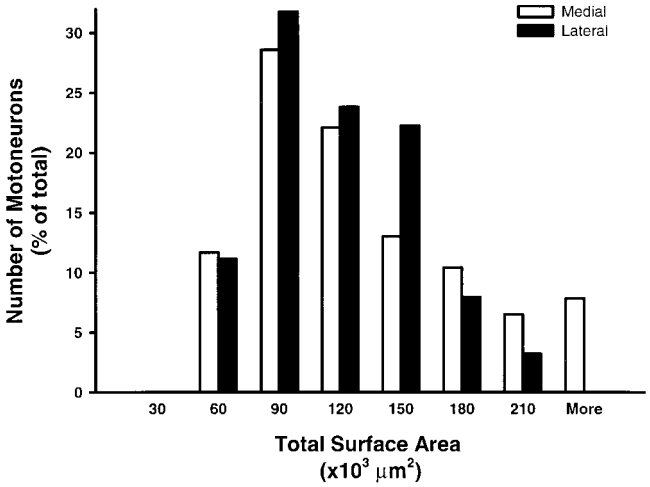

Fig. 5. Frequency distribution of estimated total membrane surface area for motoneurons innervating parasternal intercostal muscle. There are no significant differences in total motoneuron surface area between motoneurons innervating medial and lateral parasternal intercostal muscle ($P > 0.05$).

6,220 (SE) μm² for motoneurons innervating medial regions of PI muscle and 103,347 ± 4,561 μm² for lateral PI motoneurons. Medial PI motoneurons had a median total surface area of 105,860 μm², whereas that of the lateral PI motoneurons was 98,626 μm². The estimated dendritic tree surface area and total surface area (including the soma) did not vary between motoneurons innervating medial and lateral regions of PI muscle within a spinal cord segment. No differences in dendritic or total surface areas were evident across thoracic segments. Thus there were no differences in the size of motoneurons innervating different mediolateral or rostrocaudal regions of the PI muscle.

Serotonergic input to PI motoneurons. Immunoreactivity for 5-HT was extensively distributed throughout the ventral spinal cord, with single 5-HT synaptic boutons or clusters of boutons present around PI motoneuron soma and their dendrites (Fig. 6). Serotonergic terminals were also observed around unlabeled neuronal cell bodies, suggesting a wide distribution of 5-HT input to the ventral cord.

Within a thoracic segment, PI motoneurons innervating the medial region of the PI muscle displayed both a greater number and a greater density (normalized for surface area) of 5-HT boutons in the vicinity of the cell body compared with motoneurons innervating the lateral region of the muscle ($P < 0.05$; Fig. 7). In contrast, for motoneurons innervating medial or lateral regions across thoracic segments, there were no significant differences in the total number or density of 5-HT boutons around the motoneuron cell bodies (Fig. 7).

A total of 356 dendritic segments from 42 motoneurons (25 medial and 17 lateral) were analyzed for dendritic dimensions, branching order, and 5-HT input. The density of 5-HT input in the vicinity of individual dendrites ranged from 0.002 to 0.083 terminals/μm². No differences in 5-HT density were found between secondary and more distal dendrites, and thus these results were pooled for further comparisons. No difference in density of 5-HT input was found for primary and more distal dendrites of motoneurons innervating the lateral PI muscles (Fig. 8). However, the density of 5-HT input was different for primary and the more distal dendrites for motoneurons innervating the medial PI muscles ($P < 0.05$; Fig. 8). Compared with the 5-HT density at primary dendrites of motoneurons innervating medial PI muscles, there was an almost

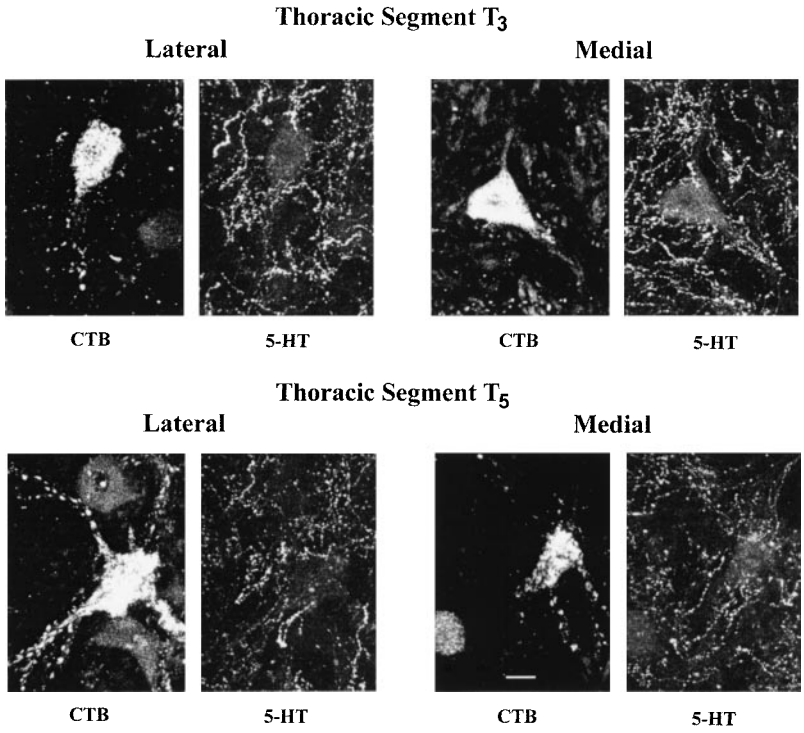

Fig. 6. Serotonergic [5-hydroxytrypamine (5-HT)] input to parasternal intercostal motoneuron somata at thoracic levels T_3 (*top*) and T_5 (*bottom*). Immunohistochemical labeling of parasternal intercostal motoneurons (CTB) and 5-HT boutons is shown. Higher density of 5-HT boutons at motoneuron somata innervating medial PI muscle compared with those innervating lateral parasternal intercostal muscle is apparent. Scale bar represents 15 μm.

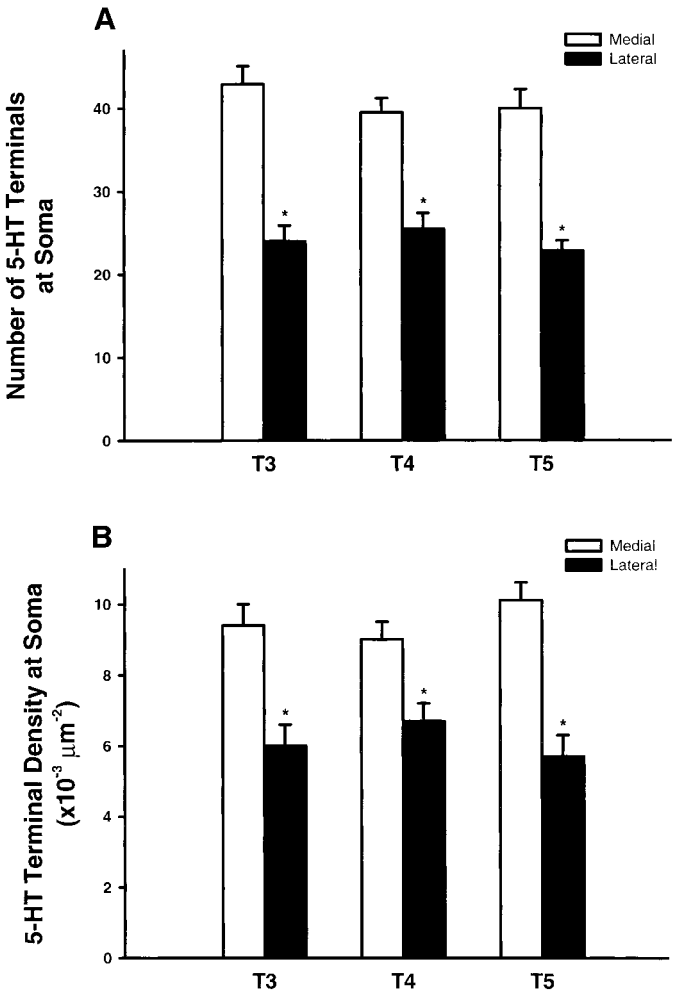

Fig. 7. Distribution of 5-HT boutons on parasternal intercostal motoneurons. Both total number (*A*) and density (*B*) of 5-HT boutons in vicinity of somata were higher in motoneurons innervating medial portion compared with lateral portion of parasternal intercostal muscles. Values are means ± SE. *Significant difference, $P < 0.05$.

twofold higher 5-HT input to second-order and more distal dendrites. The 5-HT input at distal dendrites of medial PI motoneurons was also approximately twofold higher compared with that observed at primary and distal dendrites of lateral PI motoneurons (Fig. 8).

A total of six motoneurons were traced in their entirety with complete dendritic dimensions and 5-HT terminal count, within the limitations of the system (see DISCUSSION). Detailed dendritic analyses could be obtained up to the fifth branching order in some cases. On the basis of these observations and in agreement with previous studies (2–4), the membrane surface area of primary dendrites accounted for ≃2.4% of the total dendritic surface. By using this estimate together with the measurements of 5-HT density, the total number of 5-HT terminals at primary and distal (second order and above) dendrites was determined for individual motoneurons innervating the medial and lateral PI muscles. These estimates together with measurements of the number of 5-HT terminals at the soma were used to obtain the total number of terminals per motoneuron. The estimated total number of 5-HT

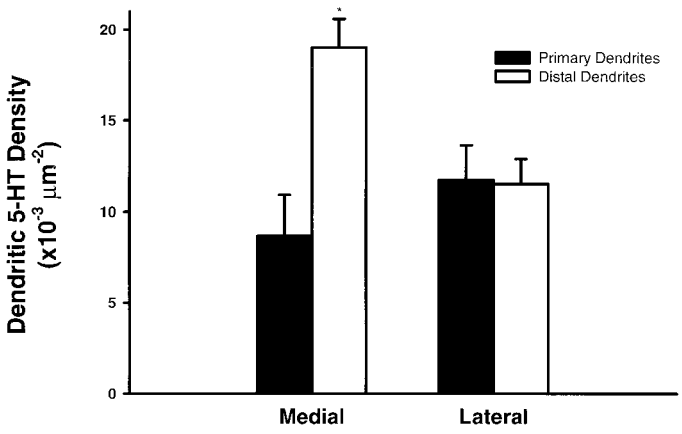

Fig. 8. Dendritic 5-HT bouton density at parasternal intercostal motoneurons. Density of 5-HT terminals was greater in secondary or higher branching order dendrites of motoneurons innervating medial portion than in primary dendrites. Similarly, distal dendrites of medial parasternal intercostal motoneurons had an almost 2-fold higher 5-HT terminal density compared with primary and more distal dendrites of lateral parasternal intercostal motoneurons. Values are means ± SE. *Significant difference, $P < 0.05$.

boutons per motoneuron ranged from 230 to 4,506. Across thoracic spinal cord segments, the total 5-HT input to motoneurons innervating the medial PI muscles was greater than that to motoneurons innervating lateral PI muscles ($P < 0.05$; Fig. 9). These results indicate that the electrophysiological evidence of graded recruitment of motoneurons innervating the PI muscles may be due, at least in part, to the existence of a mediolateral gradient in 5-HT input.

DISCUSSION

On the basis of previous studies reporting regionalization of muscle activity, i.e., spatial and temporal gradients in activation of different muscular regions, the concept of "neuromuscular partitioning" was proposed

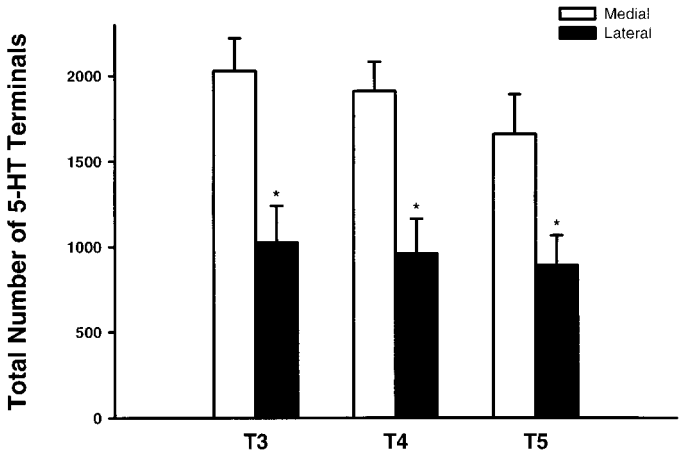

Fig. 9. Estimated total number of 5-HT terminals in vicinity of parasternal intercostal motoneurons. Total number of 5-HT boutons in vicinity of motoneuron soma and dendrites was higher in motoneurons innervating medial portion compared with lateral portion of parasternal intercostal muscles. Within individual thoracic cord segments, estimated total 5-HT terminal number was also greater in medial vs. lateral parasternal intercostal motoneurons. Values are means ± SE. *Significant difference $P < 0.05$.

(37, 39). Previous studies have suggested several potential mechanisms underlying a mediolateral recruitment pattern of PI muscles: *1*) a nonuniform spatial distribution of mechanoreceptors in the muscle leading to nonuniform activation of α-motoneuron pools by different segmental inputs, *2*) differences in the intrinsic properties of PI α-motoneurons, and *3*) differential descending synaptic input to α-motoneurons innervating different muscle regions (9, 10, 27).

The possibility that nonuniform spatial distribution of mechanoreceptor input could account for the nonuniform activation of PI muscle regions was evaluated in a recent study by De Troyer et al. (10). In dogs, a dorsal rhizotomy was performed to remove segmental afferent input to PI α-motoneurons. However, after eliminating mechanoreceptor input, these investigators found that the mediolateral gradient of PI muscle activation persisted both during normal breathing and when mechanical loading was used to increase inspiratory effort. On the basis of these data, they concluded that proprioceptive mechanisms, including muscle spindle and Golgi tendon organ reflexes, play little, if any, role in the regional activation gradient of the PI muscle.

Previous studies have demonstrated the presence of different muscle fiber types in the intercostal muscle (12, 24, 29, 33). Windhorst et al. (39) suggested that the heterogeneous distribution of muscle fiber types may reflect differential activation of motor units comprising different regions of a muscle. Accordingly, Greer and Martin (12) demonstrated a strong correlation between the activation pattern and fiber-type composition of the external intercostal muscles of the cat. However, in a recent study, De Troyer et al. (10) found no regional differences in the distribution of muscle fiber types in the canine PI muscle. Therefore, the mediolateral gradient in activation of the canine PI muscle does not appear to be correlated with gross differences in muscle fiber-type distribution. However, differences in motor unit recruitment can occur independently of motor unit type (muscle fiber type).

Morphology of PI motoneurons. The "size principle" predicts that smaller motoneurons have a lower threshold for activation than do larger motoneurons simply because of their intrinsic electrophysiological properties (13–15). In the present study, there were no differences in somal volumes, somal surface areas, dendritic surface areas, or total surface areas of motoneurons innervating medial vs. lateral regions of the canine PI muscle. Therefore,these results do not support the hypothesis that differences in intrinsic size-related electrophysiological properties of motoneurons account for the mediolateral recruitment pattern of PI muscles. However, such a conclusion assumes that the specific conductivity (conductance per unit surface area) of medial and lateral PI motoneurons is the same. Therefore, to more directly address this issue, further electrophysiological studies will be necessary.

It should be emphasized that our morphometric conclusions regarding PI motoneuron size are constrained by the limits of light microscopy. Such constraints especially apply to the analysis of the dendritic tree. By using transverse spinal cord sections, it is a daunting task to register images of dendrites from consecutive sections. Furthermore, dendrites oriented in the rostrocaudal direction were transversely sectioned. Estimates of dendritic tree size were made on the basis of the previous work by Burke et al. (1) For this calculation, dendritic surface area is estimated from measurements of the primary dendrite diameter. Primary dendrites could be easily visualized, and with an average diameter of ≃8 μm, these measurements were accurate with a <10% error. The estimates of dendritic surface for PI motoneurons are consistent with those previously reported by other investigators for α-motoneurons innervating feline phrenic motoneurons (2) and hindlimb motoneurons (3, 4).

Serotonergic synaptic input to PI motoneurons. The results of the present study demonstrated an abundance of 5-HT immunoreactive processes in the immediate vicinity of PI motoneurons. Terminal arborizations with varicosities were seen in close apposition to PI motoneuron soma and to proximal and distal dendrites, suggesting synaptic contacts with these motoneurons. Previous studies have also provided immunohistochemical evidence for 5-HT projections from raphe nuclei neurons to spinal respiratory motoneurons, including intercostal motoneurons (16, 18, 19, 25, 31, 40, 41). In the present study, we applied a stringent criterion of spatial proximity (5 μm) to maximize the likelihood that a 5-HT bouton actually modulated the juxtaposed PI motoneuron. However, by using light microscopy, it is impossible to assess whether the 5-HT boutons found in close apposition with soma or dendrites actually made synaptic contact. A potential solution to this limitation would be an electrophysiological study of individual motoneurons combined with intracellular filling of the motoneuron for morphometric analysis. On the other hand, such an approach would substantially limit the number of motoneurons that could be sampled from a single animal, a limitation overcome by the retrograde labeling technique.

In the present study, we found that 5-HT synaptic density at motoneurons innervating medial PI muscles was significantly greater than that at motoneurons innervating lateral PI muscles. A greater number and/or density of 5-HT terminals would likely result in enhanced motoneuron excitability and a lower activation threshold, which is consistent with the earlier and greater activation of motoneurons innervating the medial region of the PI muscle compared with the lateral region (9, 10). Therefore, these results support the hypothesis that descending 5-HT synaptic input modulates the activation threshold of PI motoneurons. These results are consistent with the previous suggestion that 5-HT synaptic input is critical in facilitating automatic rhythmic motor behaviors, such as respiration (21, 22), and is involved in sensory integration and facilitation of motor output (23).

These morphological data are also consistent with the considerable functional evidence for an excitatory role for 5-HT at spinal respiratory motoneurons (17, 26, 30, 35). Although most of this previous work focused on

phrenic and hypoglossal motoneurons, there is also functional evidence for a 5-HT modulation of intercostal motoneurons. Rose et al. (34) injected 5-HT into the fourth ventricle and demonstrated increased respiratory-related EMG activity of intercostal muscles. In addition, Fregosi and Mitchell (11) demonstrated that internal intercostal nerve activity (innervating PI muscles) is more sensitive to 5-HT-receptor antagonists than is phrenic nerve activity and that 5-HT-dependent long-term facilitation is also greater in PI motoneurons. Thus there is both morphological and functional evidence to suggest an excitatory role of 5-HT input in modulating PI motoneuron activity. However, these results do not exclude the possibility that other excitatory and/or inhibitory inputs also modulate the activation threshold of PI motoneurons.

The authors gratefully acknowledge the technical contributions of Yun-Hua Fang.

This work was supported by National Heart, Lung, and Blood Institute Grants HL-34817 and HL-37680, the Mayo Foundation, and Erasme University. Y. S. Prakash was supported by a fellowship from Abbott Laboratories.

Address for reprint requests and other correspondence: G. C. Sieck, Anesthesia Research, Mayo Clinic, Rochester, MN 55905 (E-mail: sieck.gary@mayo.edu).

Received 8 March 1999; accepted in final form 28 December 1999.

REFERENCES

1. **Burke RE, Marks WB, and Ulfhake B.** A parsimonious description of motoneuron dendritic morphology using computer simulation. *J Neurosci* 12: 2403–2416, 1992.
2. **Cameron WE, Averill DB, and Berger AJ.** Quantitative analysis of the dendrites of cat phrenic motoneurons stained intracellularly with horseradish peroxidase. *J Comp Neurol* 230: 91–101, 1985.
3. **Cullheim S, Fleshman JW, Glenn LL, and Burke RE.** Membrane area and dendritic structure in type-identified triceps surae alpha motoneurons. *J Comp Neurol* 255: 68–81, 1987.
4. **Cullheim S, Fleshman JW, Glenn LL, and Burke RE.** Three-dimensional architecture of dendritic trees in type-identified alpha-motoneurons. *J Comp Neurol* 255: 82–96, 1987.
5. **De Troyer A.** Inspiratory elevation of the ribs in the dog: primary role of the parasternals. *J Appl Physiol* 70: 1447–1455, 1991.
6. **De Troyer A and Cao Y.** Intercostal muscle compensation for parasternal paralysis in the dog: central and proprioceptive mechanisms. *J Physiol (Lond)* 479: 149–157, 1994.
7. **De Troyer A and Farkas GA.** Contribution of the rib cage inspiratory muscles to breathing in baboons. *Respir Physiol* 97: 135–146, 1994.
8. **De Troyer A, Farkas GA, and Ninane V.** Mechanics of the parasternal intercostals during occluded breaths in dogs. *J Appl Physiol* 64: 1546–1553, 1988.
9. **De Troyer A and Legrand A.** Inhomogeneous activation of the parasternal intercostals during breathing. *J Appl Physiol* 79: 55–62, 1995.
10. **De Troyer A, Legrand A, Gayan-Ramirez G, Cappello M, and Decramer M.** On the mechanism of the mediolateral gradient of parasternal activation. *J Appl Physiol* 80: 1490–1494, 1996.
11. **Fregosi RF and Mitchell GS.** Long-term facilitation of inspiratory intercostal nerve activity following carotid sinus nerve stimulation in cats. *J Physiol (Lond)* 477: 469–479, 1994.
12. **Greer JJ and Martin TP.** Distribution of muscle fiber types and EMG activity in cat intercostal muscles. *J Appl Physiol* 69: 1208–1211, 1990.
13. **Henneman E.** Relation between size of neurons and their susceptibility to discharge. *Science* 126: 1345–1346, 1957.
14. **Henneman E and Mendell LM.** Functional organization of motoneuron pool and its inputs. In *Handbook of Physiology. The Nervous System. Motor Control*. Bethesda, MD: Am. Physiol. Soc., 1981, sect. 1, vol. II, pt. 1, chapt. 11, p. 423–507.
15. **Henneman E, Somjen G, and Carpenter DO.** Functional significance of cell size in spinal motoneurons. *J Neurophysiol* 28: 560–580, 1965.
16. **Holtman JR.** Immunohistochemical localization of serotonin- and substance P-containing fibers around respiratory muscle motoneurons in the nucleus ambiguus of the cat. *Neuroscience* 26: 169–178, 1988.
17. **Holtman JR, Dick TE, and Berger AJ.** Involvement of serotonin in the excitation of phrenic motoneurons evoked by stimulation of the raphe obscurus. *J Neurosci* 6: 1185–1193, 1986.
18. **Holtman JR, Norman WP, Skirboll L, Dretchenk L, Cuello C, and Visser T.** Evidence for 5-hydroxytryptamine, substance P and thyrotropin-releasing hormone in neurons innervating the phrenic motor nucleus. *J Neurosci* 4: 1064–1071, 1984.
19. **Holtman JRJ, Vascik DS, and Maley BE.** Ultrastructural evidence for serotonin-immunoreactive terminals contacting phrenic motoneurons in the cat. *Exp Neurol* 109: 269–272, 1990.
20. **Izumi A and Kida MY.** Segmental distribution of the motoneurons innervating trunk muscles in the spinal cord of the cat and rat. *Neurosci Res* 30: 247–255, 1998.
21. **Jacobs BL.** Serotonin and behavior: emphasis on motor control. *J Clin Psychiatry* 52, *Suppl* 12: 17–23, 1991.
22. **Jacobs BL and Azmitia EC.** Structure and function of the brain serotonin system. *Physiol Rev* 75: 165–229, 1992.
23. **Jacobs BL and Fornal CA.** 5-HT and motor control: a hypothesis. *Trends Neurosci* 16: 346–352, 1993.
24. **Kelsen SG, Bao S, Thomas AJ, Mardini IA, and Criner GJ.** Structure of the parasternal intercostal muscles in the adult hamster: topographic effects. *J Appl Physiol* 75: 1150–1154, 1993.
25. **King KA and Holtman JRJ.** Characterization of the effects of activation of ventral medullary serotonin receptor subtypes on cardiovascular activity and respiratory motor outflow to the diaphragm and larynx. *J Pharmacol Exp Ther* 252: 665–674, 1990.
26. **Lalley PM.** Serotonergic and nonserotonergic responses of phrenic motoneurones to raphe stimulation in the cat. *J Physiol (Lond)* 380: 373–385, 1986.
27. **Legrand A, Wilson TA, and De Troyer A.** Mediolateral gradient of mechanical advantage in the canine parasternal intercostals. *J Appl Physiol* 80: 2097–2101, 1996.
28. **McCrimmon DR, Dekin MS, and Mitchell GS.** Glutamate, GABA, and serotonin in ventilatory control. In: *Regulation of Breathing* (2nd ed.), edited by Dempsey JA and Pack AL. New York: Dekker, 1995, vol. 79, p. 151–218. (Lung Biol Health Dis Se)
29. **Mizumo M and Secher NH.** Histochemical characteristics of human expiratory and inspiratory intercostal muscles. *J Appl Physiol* 67: 592–598, 1989.
30. **Morin D, Hennequin S, Monteau R, and Hilaire G.** Serotonergic influences on central respiratory activity: an in vitro study in the newborn rat. *Brain Res* 535: 281–287, 1990.
31. **Pilowsky PM, de Castro D, Llewellyn-Smith I, Lipski J, and Voss MD.** Serotonin immunoreactive boutons make synapses with feline phrenic motoneurons. *J Neurosci* 10: 1091–1098, 1990.
32. **Prakash YS, Smithson KG, and Sieck GC.** Measurements of motoneuron somal volumes using laser confocal microscopy: comparisons with shape-based stereological estimations. *NeuroImage* 1: 95–107, 1993.
33. **Reid MB, Ericson GC, Feldman HA, and Johnson RLJ.** Fiber types and fiber diameters in canine respiratory muscles. *J Appl Physiol* 62: 1705–1712, 1987.
34. **Rose D, Khater-Boidin J, Toussaint P, and Duron B.** Central effects of 5-HT on respiratory and hypoglossal activities in the adult cat. *Respir Physiol* 101: 59–69, 1995.
35. **Schmid K, Bohmer G, and Merkelbach S.** Serotonergic control of phrenic motoneuronal activity at the level of the spinal cord of the rabbit. *Neurosci Lett* 116: 204–209, 1990.

36. **Sieck GC, Mantilla CB, and Prakash YS.** Volume measurements in confocal microscopy. *Methods Enzymol* 307: 296–315, 1999.

37. **Stuart DG, Hamm TM, and Vanden Noven S.** Partitioning of monosynaptic Ia excitation to motoneurons according to neuromuscular topography. Generality and functional implications. *Prog Neurobiol* 30: 437–447, 1988.

38. **Taylor AE.** The contribution of the intercostal muscles to the effort of respiration in man. *J Physiol (Lond)* 151: 390–402, 1960.

39. **Windhorst U, Hamm TM, and Stuart DG.** On the function of muscle and reflex partitioning. *Behav Brain Sci* 12: 629–681, 1989.

40. **Yoshioka M, Ikeda T, Abe M, Togashi H, Minami M, and Saito H.** Pharmacological characterization of 5-hydroxytryptamine-induced excitation of afferent cervical vagus nerve in anesthetized rats. *Br J Pharmacol* 106: 544–549, 1992.

41. **Zhan WZ, Ellenberger HH, and Feldman JL.** Monoaminergic and GABAergic terminations in phrenic nucleus of rat identified by immunohistochemical labeling. *Neuroscience* 31: 105–113, 1989.